

Lawrence Berkeley National Laboratory

Lawrence Berkeley National Laboratory

Title

Use of TOUGHREACT to Simulate Effects of Fluid Chemistry on Injectivity in Fractured Geothermal Reservoirs with High Ionic Strength Fluids

Permalink

<https://escholarship.org/uc/item/0qg2s058>

Authors

Xu, Tianfu
Zhang, Guoxiang
Pruess, Karsten

Publication Date

2005-02-09

Use of TOUGHREACT to Simulate Effects of Fluid Chemistry on Injectivity in Fractured Geothermal Reservoirs with High Ionic Strength Fluids

Tianfu Xu, Guoxiang Zhang, and Karsten Pruess

Earth Sciences Division, Lawrence Berkeley National Laboratory
University of California, Berkeley, CA 94720
e-mail: Tianfu_Xu@lbl.gov

ABSTRACT

Recent studies suggest that mineral dissolution/precipitation and clay swelling effects could have a major impact on the performance of hot dry rock (HDR) and hot fractured rock (HFR) reservoirs. A major concern is achieving and maintaining adequate injectivity, while avoiding the development of preferential short-circuiting flow paths. A Pitzer ionic interaction model has been introduced into the publicly available TOUGHREACT code for solving non-isothermal multi-phase reactive geochemical transport problems under conditions of high ionic strength, expected in typical HDR and HFR systems. To explore chemically-induced effects of fluid circulation in these systems, we examine ways in which the chemical composition of reinjected waters can be modified to improve reservoir performance. We performed a number of coupled thermo-hydrologic-chemical simulations in which the fractured medium was represented by a one-dimensional MINC model (multiple interacting continua). Results obtained with the Pitzer activity coefficient model were compared with those using an extended Debye-Hückel equation. Our simulations show that non-ideal activity effects can be significant even at modest ionic strength, and can have major impacts on permeability evolution in injection-production systems. Alteration of injection water chemistry, for example by dilution with fresh water, can greatly alter precipitation and dissolution effects, and can offer a powerful tool for operating hot dry rock and hot fractured rock reservoirs in a sustainable manner.

1. INTRODUCTION

A major concern in the development of hot dry rock (HDR) and hot fractured rock (HFR) reservoirs is achieving and maintaining adequate injectivity, while avoiding the development of preferential short-circuiting flow paths such as those caused by thermally-induced stress cracking. Past analyses of HDR and HFR reservoirs have tended to focus primarily on the coupling between hydrology (flow), heat transfer, and rock mechanics. Recent chemistry studies suggest that rock-fluid interactions and

associated mineral dissolution and precipitation effects could have a major impact on the performance of HFR reservoirs (Jacquot, 2000; Durst, 2002; Bächler, 2003).

High ionic strength brines are expected in typical HDR and HFR systems, for which Pitzer's ionic interaction theory (Pitzer and Mayorga, 1973; Pitzer, 1991) can be used to study ionic activity in electrolytes. Ionic strength I is defined as

$$I = \frac{1}{2} \sum_i c_i z_i^2 \quad (1)$$

where the summation is over all aqueous species, and c_i and z_i are concentration (mol/kg H₂O) and electrical charge of species i , respectively.

In this study, a Pitzer ionic interaction model was introduced into the publicly available reactive transport simulator TOUGHREACT. We explored chemically-induced effects of fluid circulation in HFR systems. We examine ways in which the chemical composition of reinjected waters can be modified to improve reservoir performance by maintaining or even enhancing injectivity. We performed coupled thermo-hydrologic-chemical simulations in which the fractured medium was represented by a one-dimensional MINC model (multiple interacting continua; Pruess and Narasimhan, 1985).

2. NUMERICAL MODELING APPROACH

2.1. Computer Code

A Pitzer ionic interaction model was introduced into the reactive geochemical transport simulator TOUGHREACT (after its release to the public through the US Department of Energy's Energy Science and Technology Software Center (<http://www.osti.gov/estsc/>). Information on TOUGHREACT is available on the web at <http://www-esd.lbl.gov/TOUGHREACT>. Physical and chemical process capabilities and solution techniques of TOUGHREACT have been discussed by Xu and Pruess (2001) and Xu et al. (2004b). The simulator can be applied to one-, two-, or three-

dimensional porous and fractured media with physical and chemical heterogeneity, and can accommodate any number of chemical species present in liquid, gas and solid phases. A general form of rate law for kinetic mineral dissolution and precipitation is used. Temporal changes in porosity and permeability due to mineral dissolution and precipitation and clay swelling can modify fluid flow path characteristics. This feedback between flow and chemistry is considered in our model. The released version of TOUGHREACT uses an extended Debye-Hückel equation after Helgeson et al. (1981) for calculating activity coefficients of aqueous species, and details are given in Xu et al. (2004b). The Pitzer ionic interaction model is described below.

2.2. The Pitzer activity model

Pitzer's ionic interaction theory (Pitzer and Mayorga, 1973; Pitzer, 1991) is often used to represent ionic activity in electrolytes. The ionic activity in electrolytes is determined by the excess free energy, mostly arising from the ionic interactions of binary ionic pairs and ternary ionic combinations in the solution. Virial equations are used to quantify the excess free energy, and then the ionic activity. Harvie and Weare (1980) and Harvie et al. (1984) developed an ion-interaction equilibrium model (HMW model) for the seawater system (Na-K-Mg-Ca-Cl-SO₄-H₂O) based on Pitzer's ionic interaction theoretical model. This model is equivalent to Pitzer's original model (Pitzer and Mayorga, 1973), but different in definition of interaction coefficients and mathematical expressions (Rard and Wijesinghe, 2003). The HMW model is practically convenient for numerical implementation. The HMW model was implemented in several computer codes: PHRQPITZ (Plummer et al., 1988), UNSATCHEM-2D (Simunek and Suarez, 1994), GMIN (Felmy, 1995), and BIO-CORE^{2D} (Zhang et al., 2005). Pitzer's original model was implemented in EQ3/6 (Wolery and Daveler, 1992; Wolery et al., 2004), but from input HMW model parameters (through internal conversion).

The model implemented in TOUGHREACT is the standard HMW model (Harvie et al., 1984) using the database of Wolery et al. (2004), with user-options for simplifications dealing with solutions at different level of ionic strength. The most simplified version is the Debye-Hückel model that does not account for any ionic interaction terms and generally is only applicable to solutions with ionic strength less than 1 M. It has already been used in the released version of TOUGHREACT (Xu and Pruess, 2001; Xu et al., 2004b).

The Pitzer activity model in TOUGHREACT accounts for interaction terms of cation-anion, cation-neutral, anion-neutral, cation-anion-anion, cation-

cation-anion, neutral-cation-anion, neutral-cation-cation and neutral-anion-anion interaction terms. When dealing with reactive transport problems for a given solution with a pre-estimated ionic strength range, simplifications may be made for a significant saving of computational time without losing accuracy. It has been shown that with only binary (cation-anion, cation-neutral, anion-neutral) terms, the HMW model is applicable to solutions with ionic strength lower than 7 M (Zhang et al., 2005). All equations in the HMW model (Harvie et al., 1984) related to water activity, osmotic coefficient, activity coefficients of cations, anions, and neutral species are summarized in Zhang et al. (2005).

3. PROBLEM SETUP

3.1. Mineralogical Condition

We consider three different mineral assemblages (Table 1). The first represents strongly altered minerals from a highly fractured vein, and includes minerals from the original granite (mainly quartz) that are fully cemented by clays, carbonates, and secondary quartz veins. The second assemblage is composed of altered granite blocks partly cemented by alteration products that consist essentially of clay minerals and carbonates. The third is the unaltered granite in which the fracture density is close to zero. Mineral dissolution and precipitation are considered under kinetic constraints. A general kinetic rate expression is used in TOUGHREACT (Xu et al., 2004b). Kinetic parameters are taken from Xu and Pruess (2004).

Table 1. Initial mineralogical composition of the three zones used in the simulations. Data were taken from Jacquot (2000), Durst (2002), and Bächler (2003).

Mineral	Volume percentage of solid rock		
	Fractured vein Alteration	Altered granite	Unaltered granite
Quartz	43.9	4.09	24.2
K-feldspar		13.9	23.6
Plagioclase			42.5
Biotite			4.2
Hornblende			3.1
Chlorite		4.8	2
Calcite	4.3	3.3	0.3
Dolomite	0.7	0.8	
Illite	40.2	24.6	
Na-smectite	7.392	7.469	
Ca-smectite	2.208	2.231	
Pyrite	1	0.7	
Galena	0.3	1.3	
Non-reactive		36.81	0.1

3.2. Fluid flow conditions

A one-dimensional MINC (multiple interacting continua) model was used to represent the fractured rock (Figure 1). Subgrid 1 represents the fracture vein alteration, while subgrids 2 and 3 represent the altered and unaltered granite, respectively. The MINC method can resolve “global” flow and diffusion of chemicals in the fractured rock and its interaction with “local” exchange between fractures and matrix. Details on the MINC method for reactive geochemical transport are described by Xu and Pruess (2001).

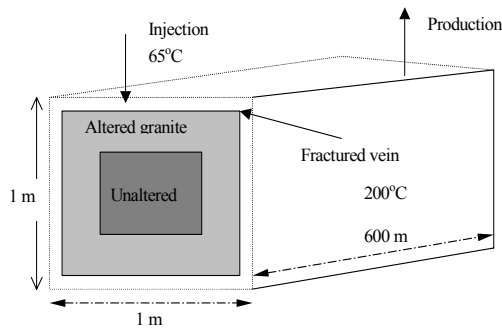


Figure 1. Subgridding of a matrix in the “multiple interacting continua” (MINC) method. The figure represents a view of a rock matrix column that is bounded by fractures.

We used an idealized fractured porous medium with two perpendicular sets of planar, parallel fractures of equal aperture and spacing. Because of the assumed symmetry only one column of matrix blocks needs to be modeled. Our conceptual model considers a one-dimensional flow tube between injection and production well, which should be considered as a small sub-volume of a much more extensive 3-D reservoir. From the injection side to the production side, the model consists of 72 grid blocks representing 600 m distance. The block size gradually increases from 0.1 m at the injection side to 20 m at the production side.

Hydrological parameters used in the present simulations are listed in Table 2. Notice that some are different from those of Durst (2002) and Bächler (2003). For example, previous investigators used a permeability of $1 \times 10^{-11} \text{ m}^2$ and a porosity of 0.1 for the fractured vein. The objective of the present study is to explore methods for minimizing mineral scaling and clay swelling, mitigating injection water chemistry, and preserving or enhancing injectivity.

Even though we took some data from the European HDR site as a starting point, we attempted to use thermophysical conditions and parameters that could represent general geothermal reservoirs. Initial reservoir temperature and pressure were 200°C and 50 MPa, respectively. An over-pressure of 2 MPa was applied at the injection (left) side, and was held constant over time. Injected water temperature was taken as 65°C. Conductive heat exchange with the surrounding low-permeability rock is an important process, and is treated with a semi-analytical technique developed by Vinsome and Westerveld (1980). In the present simulations, chemical interactions in the unaltered granite zone were not considered. This does not significantly affect chemical changes in the fractured vein because of the extremely low permeability of the granite.

Table 2. Hydrogeologic and thermal parameters used for the three mineralogical zones (a density of 2650 kg.m^{-3} , a heat capacity of $1000 \text{ J.kg}^{-1}\text{K}^{-1}$, and an diffusivity of $1 \times 10^{-9} \text{ m}^2.\text{s}^{-1}$ were used for all three zones).

Parameters	Fractured vein	Altered granite	Unaltered granite
Volume	10%	60%	30%
Permeability (m^2)	2×10^{-12}	2×10^{-15}	2×10^{-18}
Porosity	0.2	0.1	0.02
Thermal conductivity ($\text{W.m}^{-1}\text{K}^{-1}$)	2.9	3	3
Tortuosity	0.3	0.1	0.05

3.3. Water chemistry

We started with a 165°C water sample taken from Soultz Well GPK1 at 3500 m depth (Table 3). Initial water chemical compositions for the fractured vein and altered granite zones were obtained by equilibrating the sample water with their corresponding mineral compositions (Table 1) at a temperature of 200°C.

Two types of injection waters with different chemical compositions were considered in the present simulations, and were held constant over time. The first type corresponded to the native water in the fractured vein zone but with a lower temperature of 65°C, which should be close to the produced reservoir water without surface treatment (base case). The second injection water was obtained by diluting the native water by a factor of 2 (i.e., one unit of reservoir water was mixed with one unit of fresh water; mixing case).

Table 3. List of water chemical concentration (mol/l) of Soultz Well GPK1 sample (Durst, 2002). No measurements for Fe, Al, and Pb concentrations in the sample were reported, and small values were assumed for consistency because of the presence of minerals with these components.

Chemical components	Soultz Well GPK1 at 3500 m depth (165°C)
Ca	1.820×10^{-1}
Mg	4.610×10^{-3}
Na	1.213
K	7.180×10^{-2}
Fe	1.491×10^{-6}
Cl	1.72
SiO ₂ (aq)	3.500×10^{-3}
HCO ₃	7.500×10^{-3}
SO ₄	2.020×10^{-3}
Al	5.656×10^{-9}
Pb	1.000×10^{-12}
pH	5.03
I (ionic strength)	1.8834

3.4. Simulation setup

A total of four simulations were performed using the two different types of injection waters mentioned above (base and mixing cases) for each activity model, Pitzer and Debye-Hückel (DH). The native reservoir water has an ionic strength (I) equal to 1.8834, the mixing case injection water has an I of 0.9417. The minimum ionic strength I_{\min} (Eq. A.2 in Appendix A) to maintain clay density is dependent on the type of clays, type of salts dissolved in water, and temperature and pressure conditions. In the present simulations, we simply selected $I_{\min} = 1.5$, which is slightly below the I of the native reservoir water. The maximum density reduction factor f_{\max} is also a predetermined parameter. Experiments on compacted bentonite showed that density could be reduced due to swelling by 26% (JNC, 2003). Studies conducted by Newman (1987) and de Siqueira et al. (1999) indicated that the layer spacing in dry clays is about 9.8 Å. If one assumes that the diameter of a water molecule is 2.7 Å, clay hydrates containing one, two, and three molecular layers of water will have a spacing of around 12.5, 15.2 and 17.9 Å. In the reservoir, the clay may not be well contacted by the injected water and conditions could be different from the lab. We used a maximum density reduction factor $f_{\max} = 5\%$.

The Verma and Pruess porosity-permeability relationship (Appendix B) used requires two parameters, one is the “critical” porosity ϕ_c , and the other is n , a power law exponent. In the present

simulations, we used a ϕ_c of 0.16 (80% of initial porosity of 0.2 for the fractured vein), and an n of 2. A ϕ_c of 80% initial porosity is quite reasonable and may be conservative. Precipitation and dissolution of all minerals were modeled as kinetic processes.

4. RESULTS AND DISCUSSION

4.1. Base case

The 65°C injection water is under-saturated with respect to calcite because this water was in equilibrium with reservoir rock at 200°C. Significant calcite dissolves close to the injection side because calcite solubility decreases with temperature (Figure 2). As temperatures increase away from the injection point, calcite becomes over-saturated and precipitation occurs. Areas of calcite dissolution and precipitation move gradually away from the injection point due to changes in temperature along the flow path. A maximum of about 4% volume of calcite has been precipitated after three years. Dolomite also dissolves close to the injection side but later precipitates, and quartz precipitation occurs (no amorphous silica precipitation is observed for this range of temperatures). The amounts of dolomite and quartz precipitation are about one order of magnitude smaller than calcite. Some pyrite and galena precipitation, and very slight illite and smectite precipitation occur near the injection point. Notice that amounts of precipitation and the distribution depend on their precipitation kinetics.

Changes in porosity due to mineral dissolution and precipitation (mainly calcite) are presented in Figure 3. Porosity increases indicate that mineral dissolution is dominant, while porosity decreases when precipitation dominates. The dissolved ions from calcite dissolution close to the well are transported along the flow path, and then induce precipitation at further distance from the well. If we used a 1-D radial model, calcite precipitation would spread over a much larger area than in the 1-D column model.

Figure 4 shows the time dependence of injection (flow) rate. The way in which flow gets reduced from precipitation reduces porosity towards the critical value (Appendix B). As flow rate decline, temperatures increase, causing additional calcite precipitation and further injectivity decrease. This is because calcite has retrograde solubility (is less soluble at higher temperatures), which makes this mineral prone to precipitation from reinjected waters as they are being heated in the reservoir.

Results obtained from the Pitzer and Debye-Hückel activity coefficient models are different, which can be clearly seen in Figures 2-4. In the Pitzer model, a minimum porosity due to calcite precipitation

develops at 30 m from the well after three year of injection. The injection rate is close to zero (Figure 4). In actual field operation, the injection would stop before that.

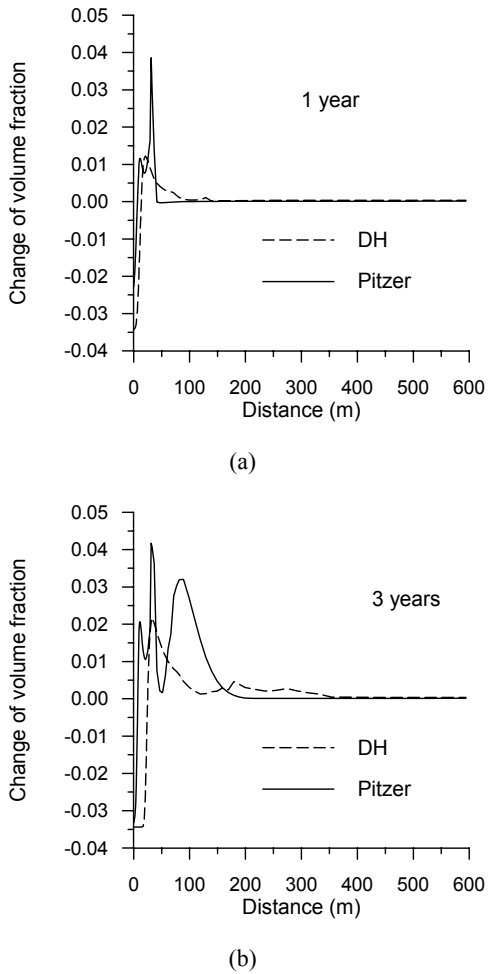


Figure 2. Changes of calcite abundance (given in reservoir volume fractions) obtained from the base case.

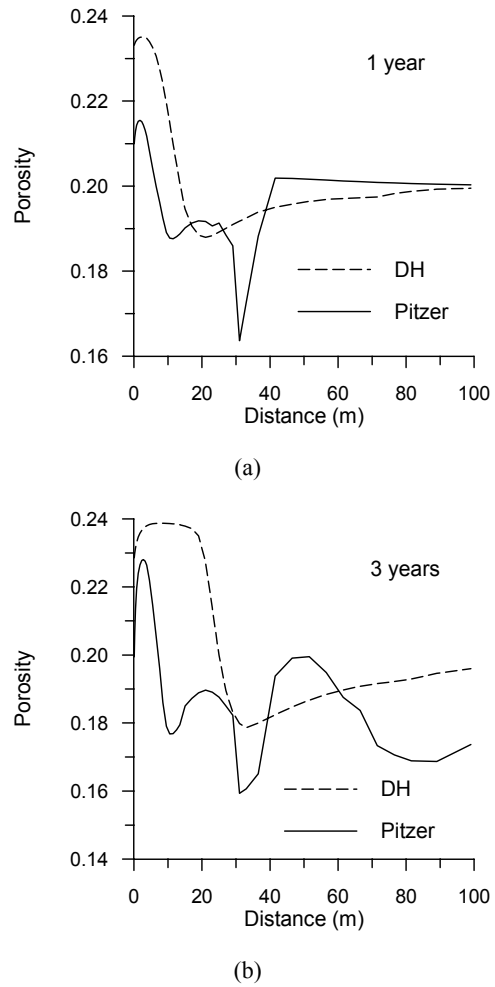


Figure 3. Distribution of porosity obtained from the base.

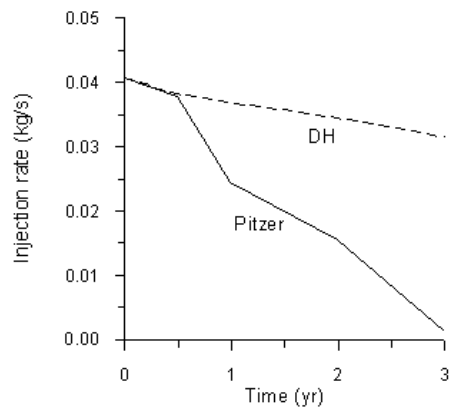
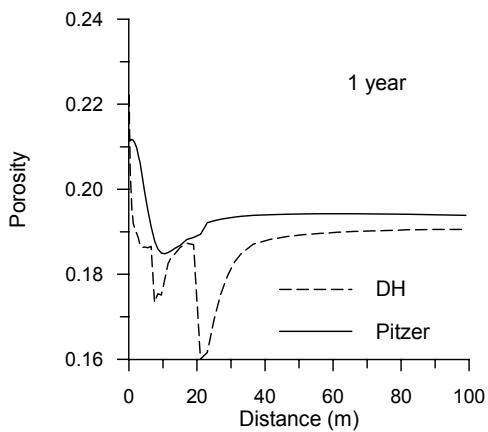


Figure 4. Injection rate (kg/s) over time of the fracture-matrix column with an area of 1 m^2 obtained from different simulations.

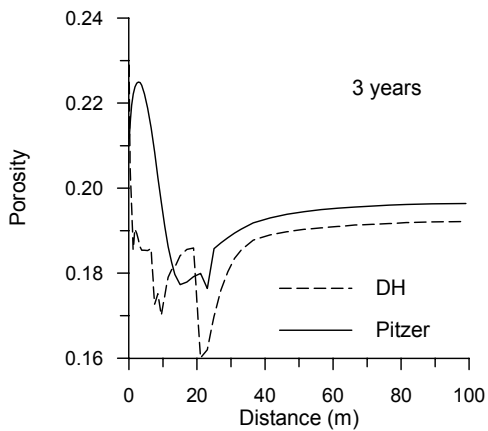
4.2. Mixing case

The mixing case injection water (with an $I = 0.93315$) causes the clay swelling that contributes a porosity decrease of about 0.01 along the entire flow path. Note that the extent of porosity decrease depends upon the minimum ionic strength I_{\min} and the maximum density reduction factor f_{\max} (Eq. A.2 in Appendix A).

For the Pitzer model, the mixing injection water is favorable for porosity development and maintaining injectivity. In contrast to the base case, the Debye-Hückel model results in a minimum porosity due to calcite precipitation at 20 m from the well after three years, and then an injection rate close to zero. Once again, we should note that if a 1-D radial model was used, calcite precipitates would spread over a larger area than in the 1-D column model, resulting in less porosity decreases.



(a)



(b)

Figure 5. Distribution of porosity obtained from the mixing case.

4.3. Discussion

For the base case with an ionic strength (I) of 1.8834, the result of the Debye-Hückel model is quite different from that of the Pitzer model. As mentioned before the Debye-Hückel model does not account for any ionic interaction terms and generally is only applicable to solutions with I less than 1 M. Figure 6 shows the measured and calculated mean activity coefficients of $NaCl$. The mean coefficient γ_{NaCl} is calculated as $\ln\gamma_{NaCl} = (\ln\gamma_{Na} + \ln\gamma_{Cl})/2$, where γ_{Na} and γ_{Cl} activity coefficients of Na^+ and Cl^- , respectively. For $I > 1$ M, the extended Debye-Hückel models deviates from the Pitzer model.

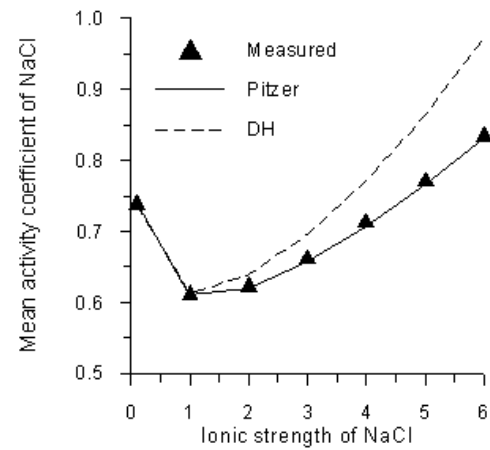


Figure 6. Mean activity coefficient of $NaCl$ vs. ionic strength of $NaCl$ solution. Measured data were taken from Colin et al. (1985)

Calcite solubility ($CaCO_3 + H^+ = Ca^{+2} + HCO_3^-$) depends on ion activities according to

$$K = \gamma_{Ca^{+2}} C_{Ca^{+2}} \gamma_{HCO_3^-} C_{HCO_3^-} / \gamma_{H^+} C_{H^+} \quad (2)$$

where K is the solubility (equilibrium) constant, C is concentration of aqueous species (mol/kg H_2O). At high ionic strength and high temperature, activity coefficients of Ca^{+2} calculated from the Pitzer model are much larger than from the Debye-Hückel. This means a lower Ca^{+2} concentration is needed to maintain calcite equilibrium or calcite is less soluble. The effect of increased Ca^{+2} activity coefficients on calcite solubility in this case is similar to the “salting out” effects for dissolution of non-condensable gases such as CO_2 .

5. SUMMARY AND CONCLUSIONS

A total of four simulations have been performed using the produced reservoir and the mixing waters for each activity model, Pitzer and Debye-Hückel. For the case of directly using the produced reservoir water, the Pitzer model predicted more calcite precipitation and a precipitation peak is developed at

30 m from the well. The mixing water causes a porosity decrease close to 0.01 due to clay swelling along the entire flow path for both models. However, the Pitzer model results in less calcite precipitation than the Debye-Hückel, indicating that calcite is more soluble at one half of the ionic strength of the reservoir water. Overall, the effect of less calcite precipitation (over clay swelling) is dominant. The Pitzer model suggests that the mixing injection water is favorable for porosity development and maintaining injectivity. We should note that if a 1-D radial model was used, calcite precipitation would spread over a much larger area than for the 1-D column model, resulting in less porosity decreases.

The Debye-Hückel model deviates increasingly from the Pitzer one at elevated temperatures and at high ionic strength greater than 1 M. Because high temperature and high ionic strength water are encountered in geothermal reservoirs, the Pitzer model should be used.

Calcite has retrograde solubility (is less soluble at higher temperatures), which makes this mineral prone to precipitation from reinjected waters as they are being heated in the reservoir. Such precipitation will reduce porosity and may have major detrimental impacts on permeability. Most minerals are more soluble at higher temperatures, tending to dissolve as injected waters are being heated. Precipitation and dissolution effects depend sensitively on concentrations and activities of participating ionic species. Our simulations show that non-ideal activity effects can be significant even at modest ionic strength, and can have major impacts on permeability evolution in injection-production systems. Alteration of injection water chemistry, for example by dilution with fresh water, can greatly alter precipitation and dissolution effects, and can offer a powerful tool for operating hot dry rock and hot fractured rock reservoirs in a sustainable manner.

The reaction kinetics of mineral alteration and the relationship between porosity and permeability changes are uncertain. Sensitivity studies should be performed in the future. The well configuration and data for mineralogical composition in this study were taken from the European HDR research site, but the results and conclusions should be useful for other HFR reservoirs, because calcite is commonly present in geothermal systems.

ACKNOWLEDGEMENTS

We are grateful to Nicolas Spycher and Chao Shan for suggestions for improvement of this manuscript. This work was supported by the Assistant Secretary for Energy Efficiency and Renewable Energy, Office of Geothermal Technologies, of the U.S. Department

of Energy, under Contract No. DE-AC03-76SF00098.

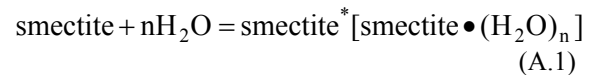
REFERENCES

- Bächler, D., 2003. Coupled thermal-hydraulic-chemical modeling at the Soultz-sous-Forêts HDR reservoir (France). PhD dissertation, Swiss Federal Institute of Technology, Zurich, Switzerland.
- Colin, E., W. Clarke, and D. N. Glew, 1985, Evaluation of the thermodynamic functions for aqueous sodium chloride from equilibrium and calorimetric measurements below 154°C, *J. Phys. Chem. Ref. Data*, Vol.14, No.2, 489-541.
- de Siqueira, A.V., Lobban, C., Skipper, N.T., Williams, G.D., Soper, A.K., Done, R., Dreyer, J.W., Humphreys, R.J., and Bones, J.A.R., 1999. The structure of pore fluids in swelling clays at elevated pressures and temperatures. *J. Phys.: Condens. Matter* 11, 9179-9188.
- Durst, D., 2002. *Geochemical modeling of the Soultz-sous-Forêts Hot Dry Rock test site: Coupled fluid-rock interaction to heat and fluid transport*. PhD dissertation, Université de Neuchâtel, France.
- Felmy, A. R., 1995, GMIN, A computerized chemical equilibrium program using a constrained minimization of the Gibbs free energy: Summary report, Soil Science Society of America, Special publication, 42, 377-407.
- Harvie, C. E., and J. H. Weare, 1980, The prediction of mineral solubilities in natural waters: The Na-K-Mg-Ca-Cl-SO₄-H₂O system from zero to high concentration at 25 °C, *Geochim. Cosmochim. Acta*, 44(7), 981-997.
- Harvie, C. E., N. Moller, and J. H. Weare, 1984. The prediction of mineral solubilities in natural waters: The Na-K-Mg-Ca-H-Cl-SO₄-OH-HCO₃-CO₃-H₂O-system to high ionic strengths at 25 °C. *Geochim. Cosmochim. Acta*, 48(4), 723-751.
- Helgeson, H.C., D.H. Kirkham, and D.C. Flowers, Theoretical prediction of the thermodynamic behavior of aqueous electrolytes at high pressures and temperatures: IV. Calculation of activity coefficients, osmotic coefficients, and apparent molal and standard and relative partial molal properties to 600 C and 5 kb. *Am. J. Sci.*, v. 281, p. 1249-1516, 1981.
- Jacquot, E., 2000. *Modélisation thermodynamique et cinétique des réactions géochimiques entre fluides de bassin et socle cristalline. Application au site expérimental du programme européen de recherché en géothermie profonde (Soultz-sous-Forêts, Bas Rhin, France)*. PhD dissertation, Univ. Louis Pasteur, Strasbourg, France.
- JNC (Japan Nuclear Cycle Development Institute), 2003. Repository Design and Engineering Technology. Technical Report.
- Malmstrom M., S. Banwart, J. Lewenhagen, L. Duro, and J. Bruno, 1996. The dissolution of biotite and

- chlorite at 25°C in the near-neutral pH region. *Contaminant Hydrology*, 21, 201-213.
- Newman, A.C.D., 1987. *Chemistry of Clays and Clay Minerals* (London: Mineralogical Society).
- Pitzer, K.S., and G. Mayorga, 1973. Thermodynamics of electrolytes. II. Activity and osmotic coefficients for strong electrolytes with one or both ions univalent. *J. Phy. Chem.*, 77, 2300-2307.
- Pitzer, K.S., 1991. Ion interaction approach: Theory and data correlation. In: *Activity Coefficients in Electrolyte Solutions*, edited by K. S. Pitzer, 2nd ed., CRC Press, 75-155.
- Plummer, L. N., D. L. Parkhurst, G. W. Fleming, and S. A. Dunkle, 1988, *A Computer Program Incorporating Pitzer's Equations for Calculation of Geochemical Reactions in Brines*, USGS Water Resources Investigation Report 88-4153, 1-310.
- Pruess, K., and T.N. Narasimhan, A practical method for modeling fluid and heat flow in fractured porous media: *Society of Petroleum Engineers Journal*, 25, 14-26, 1985.
- Rard J.A., Wijesinghe, A.M., 2003. Conversion of parameters between different variants of Pitzer's ion-interaction model, both with and without ionic strength dependent higher-order terms. *J. Chem. Thermodynamics*, 35, 439-473.
- Simunek, J., and L. Suarez, 1994, Two-dimensional transport model for variably saturated porous media with major ion chemistry, *Water Resour. Res.*, 30(4), 1115-1131.
- Verma, A., and K. Pruess, 1988. Thermohydrological conditions and silica redistribution near high-level nuclear wastes emplaced in saturated geological formations. *J. Geophys. Res.*, 93, 1159-1173.
- Vinsome, P. K. W., and J. Westerveld, 1980. A simple method for predicting cap and base rock heat losses in thermal reservoir simulators. *J. Canadian Pet. Tech.*, 19 (3), 87-90.
- Wolery T. J., and S. A. Daveler, 1992, *EQ6, A Computer program for Reaction Path Modeling of Aqueous Geochemical System: Theoretical Manual, User's Guide, and Related Documentation (version 7.0)*, Lawrence Livermore National Laboratory, UCRL-MA-110662 PT IV.
- Wolery T., Jove-Colon C., Rard, J., Wijesinghe, A., 2004. Pitzer Database Development: Description of the Pitzer Geochemical Thermodynamic Database data0.ypf. Appendix I in *In-Drift Precipitates/Salts Model (P. Mariner)* Report ANL-EBS-MD-000045 REV 02. Las Vegas, Nevada: Bechtel SAIC Company.
- Xu, T., and K. Pruess, 2001. Modeling multiphase non-isothermal fluid flow and reactive geochemical transport in variably saturated fractured rocks: 1. Methodology. *Am. J. Sci.*, 301, 16-33.
- Xu, T., and K. Pruess, Numerical simulation of injectivity effects of mineral scaling and clay swelling in a fractured geothermal reservoir, Proceedings of Geothermal Resources Council 2004 Annual Meeting (Vol 28 of *GRC Transactions*), Palm Springs, California, August 29-September 1, 2004.
- Xu, T., Y. Ontoy, P. Molling, N. Spycher, M. Parini, K. Pruess, 2004a. Reactive transport modeling of injection well scaling and acidizing at Tiwi Field, Philippines. *Geothermics*, 33(4), 477-491.
- Xu, T., E. Sonnenthal, N. Spycher, and K. Pruess, 2004b. *TOUGHREACT user's guide: A simulation program for non-isothermal multiphase reactive geochemical transport in variable saturated geologic media*, Lawrence Berkeley National Laboratory Report LBNL-55460, Berkeley, California, 192 pp.
- Zhang G. Z. Zheng, and J. Wan, 2005. Modeling Geochemical Reactive Transport of Concentrated Aqueous Solution, *Water Resour. Res.*, in press.

APPENDIX A. CLAY SWELLING

Swelling clays such as smectite and illite are layered minerals made up of negatively charged mica-like sheets, which are held together by charge-balancing interlayer cations such as Ca^{2+} , Mg^{2+} , or Na^+ (de Siqueira et al., 1999). These cations adsorb water molecules, and water films form on clay surfaces. An increase of solution ionic strength causes a reduction of the thickness of the bonded water film (shrinking). When the clay is contacted by aqueous solutions of low ionic strength, the thickness will increase and clay will swell. Using smectite as an example, this process can be schematically formulated as



where smectite* is the swelled bulk clay with bonded water films. As water activity increases when diluting a solution of high ionic strength, the reaction (A.1) would be driven to the right. This will result in a decrease in bulk density of the clay, and consequently a reduction in porosity and permeability. The detailed mechanism of clay swelling (shrinking) is very complex. In the present study, we use a simple approach calculating the bulk clay density by

$$\rho = \rho_{\max} \left[1 - f_{\max} \frac{I_{\min} - I}{I_{\min}} \right] \quad I < I_{\min}$$

$$\rho = \rho_{\max} \quad I \geq I_{\min} \quad (\text{A.2})$$

where ρ_{\max} is the maximum clay density achieved when ionic strength I exceeds a certain minimum value I_{\min} , and f_{\max} is the maximum density reduction factor when $I = 0$.

APPENDIX B. CHANGES OF PERMEABILITY

Temporal changes in porosity and permeability due to mineral dissolution and precipitation and clay swelling can modify fluid flow path characteristics. This feedback between flow and chemistry is considered in our model. Changes in porosity are calculated from changes in mineral volume fractions. Four different porosity-permeability relationships were coded in TOUGHREACT, including the Kozeny-Carman grain model and the Verma and Pruess model (1988). In the present work, we used a relationship of Verma and Pruess (1988), with a more sensitive coupling of permeability to porosity than the Kozeny-Carman relationship

$$\frac{k}{k_0} = \left(\frac{\phi - \phi_c}{\phi_0 - \phi_c} \right)^n \quad (\text{B.1})$$

where ϕ_c is the “critical” porosity at which permeability goes to zero, and n is a power law exponent. Eq. (B.1) is derived from a pore-body-and-throat model in which permeability can be reduced to zero with a finite (“critical”) porosity remaining. Parameters ϕ_c and n are medium-dependent. The relationship of Verma and Pruess (1988) was found to better capture injectivity losses (Xu et al., 2004a).